IEEJ Journal of Industry Applications
Vol.7 No.2 pp.127–140 DOI: 10.1541/ieejjia.7.127

Paper

Advanced Motion Control for Precision Mechatronics: Control, Identification, and Learning of Complex Systems

Tom Oomen[*a)] Non-member

(Manuscript received May 4, 2017, revised Aug. 8, 2017)

Manufacturing equipment and scientific instruments, including wafer scanners, printers, microscopes, and medical imaging scanners, require accurate and fast motions. An increase in such requirements necessitates enhanced control performance. The aim of this paper is to identify several challenges for advanced motion control originating from these increasing accuracy, speed, and cost requirements. For instance, flexible mechanics must be explicitly addressed through overactuation, oversensing, inferential control, and position-dependent control. This in turn requires suitable models of appropriate complexity. One of the main advantages of such motion systems is the fact that experimenting and collecting large amounts of accurate data is inexpensive, paving the way for identifying and learning of models and controllers from experimental data. Several ongoing developments are outlined that constitute part of an overall framework for control, identification, and learning of complex motion systems. In turn, this may pave the way for new mechatronic design principles, leading to fast lightweight machines where spatio-temporal flexible mechanics are explicitly compensated through advanced motion control.

Keywords: mechatronics, motion control, robust control, multivariable control, system identification, iterative learning control

1. Introduction

Positioning systems are a key enabling technology in manufacturing machines and scientific instruments. A state-of-the-art example of such a mechatronic system is a wafer scanner, which is used in the lithographic production of integrated circuits (ICs), see Figs. 1(a)–1(b), and achieves sub-nanometer positioning accuracy with extreme speed and acceleration [(1)]. Also, in semiconductor assembly processes, including wire bonders and die bonders, see Fig. 1(c), products have to be positioned with varying trajectories, up to 72000 products per hour [(2)]. Furthermore, for printing systems, ranging from desktop printers to industrial printers and 3D printing, see Fig. 1(d), printing accuracy and speed are essential. In scientific instruments, such as atomic force microscopes (AFMs) and scanning electron microscopes (SEM), the sample needs to be accurately positioned [(3)(4)], whereas in computed tomography CT scanners the detector is positioned for medical imaging, see Fig. 1(e). The accuracy and speed of these positioning systems hinges on the motion control design [(5)–(7)] and determines the capabilities and market position of the manufacturing machines and scientific instruments.

Control of these positioning systems is traditionally simplified by an excellent mechanical design. In particular, the mechanical design is such that the system is stiff and highly reproducible. In conjunction with moderate performance requirements, the control bandwidth is well-below the resonance frequencies of the flexible mechanics, as is also schematically shown in Fig. 2(a). As a result, the system can often be completely decoupled [(8)] in the frequency range relevant for control. Consequently, the control design is divided into well-manageable single-input single-output (SISO) control loops, for which standard guidelines exist for their manual tuning by control engineers for both feedback and feedforward, see [(7)(9)–(11)] and Sec. 2.2. In addition, SISO learning control approaches that are suitable for motion control are well-developed, see [(12)(13)].

Although motion control design is well-developed, presently available techniques mainly apply to positioning systems that behave as a rigid body in the relevant frequency range. On the one hand, increasing performance requirements hamper the validity of this assumption, since the bandwidth, i.e., the frequency range over which control is effective, has to increase, leading to flexible dynamics in the cross-over region, see Fig. 2(b) and also [(14)–(16)]. On the other hand, the requirement for rigid-body behavior puts high requirements on the mechatronic system design, e.g., in terms of exotic and stiff materials and hence cost.

The aim of this paper is to sketch the present state of the practice (Sec. 2) and to identify challenges arising in precision motion control (Sec. 3). Recent results that address these challenges in motion feedback control are outlined (Sec. 4), revealing the need for system identification techniques. Next, feedforward and learning control are addressed (Sec. 5). Hence, this paper addresses both feedback, identification, feedforward, and learning, extending the earlier papers [(17)–(19)]. Finally, an outlook on ongoing and related developments in provided (Sec. 6).

2. Traditional Motion Control

2.1 Motion Systems Mechatronic positioning systems consist of mechanics, actuators, and sensors [(9)(20)]. The

a) Correspondence to: Tom Oomen. E-mail: t.a.e.oomen@tue.nl
* Eindhoven University of Technology, Department of Mechanical Engineering
Eindhoven, The Netherlands

(a) Experimental wafer stage.

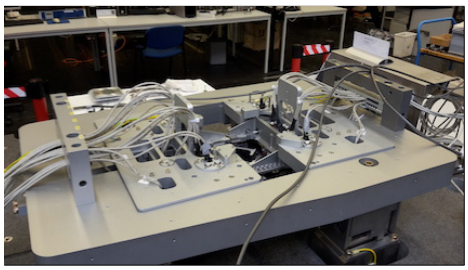

(b) Prototype reticle stage.

(c) Wire bonder.

(d) Industrial flatbed printer.

(e) CT scanner.

Fig. 1. Example state-of-the-art positioning systems

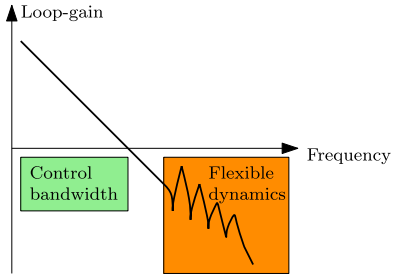

(a) Traditional loop-gain.

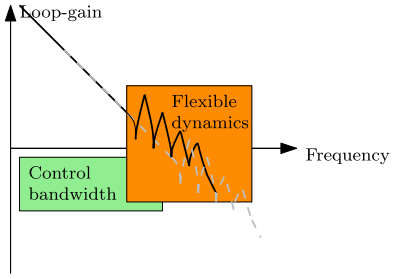

(b) Envisaged loop-gain in next-generation systems.

Fig. 2. Envisaged developments in motion systems. In traditional motion systems, the control bandwidth, i.e., the frequency where the loop-gain crosses 0 dB takes place in the rigid-body region. In next-generation systems, flexible dynamics are foreseen to occur within the control bandwidth. Indeed, on the one hand, increasing performance requirements necessitate a larger bandwidth. On the other hand, lightweight constructions lead to the occurrence of flexible dynamics at lower frequencies

actuators typically generate forces and are considered as input to the system. The sensors typically measure position and are considered as output of the system.

In the frequency range that is relevant for control, the dynamical behavior is mainly determined by the mechanics. In particular, the mechanics can typically be described as [21]–[23]

$$G_m = \underbrace{\sum_{i=1}^{n_{RB}} \frac{c_i b_i^T}{s^2}}_{\text{rigid-body modes}} + \underbrace{\sum_{i=N_{rb}+1}^{n_s} \frac{c_i b_i^T}{s^2 + 2\zeta_i \omega_i s + \omega_i^2}}_{\text{flexible modes}}, \cdots\cdots (1)$$

where n_{RB} is the number of rigid-body modes, the vectors $c_i \in \mathbb{R}^{n_y}$, $b_i \in \mathbb{R}^{n_u}$ are associated with the mode shapes, and $\zeta_i, \omega_i \in \mathbb{R}_+$. Here, $n_s \in \mathbb{N}$ may be very large and even infinite [24]. Note that in (1), it is assumed that the rigid-body modes are not suspended, i.e., the term $\frac{1}{s^2}$ relates to Newton's law. In the case of suspended rigid-body modes, e.g., in case of flexures as in [10][25], (1) can directly be extended.

In traditional positioning systems, the number of actuators n_u and sensors n_y equals n_{RB}, and are positioned such that the matrix $\sum_{i=1}^{n_{RB}} c_i b_i^T$ is invertible. In this case, matrices T_u and T_y can be selected such that

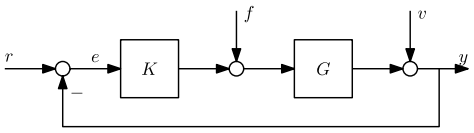

Fig. 3. Traditional motion control architecture

$$G = T_y G_m T_u = \frac{1}{s^2} I_{n_{RB}} + G_{\text{flex}}, \cdots\cdots (2)$$

where T_y is typically selected such that the transformed output y equals the performance variable z, as is defined in Sec. 3.3. Importantly, the selection of these matrices T_u and T_y can be done directly on the basis of frequency response function (FRF) data, e.g., [8]. Such frequency response data is inexpensive, fast, and accurate to obtain. The importance of such frequency response data is further clarified in Sec. 4.8.

2.2 Traditional Control Architecture The motion control architecture in Fig. 3 is standard, where

$$e = S(r - Gf) - Sv, \cdots\cdots (3)$$

with $S = (I + GK)^{-1}$. Typically, r is a prespecified reference trajectory for the output y, e is the vector of error signals to be minimized, f is a feedforward signal, K is the feedback

controller, and v represents disturbances. It is remarked that these are tacitly used for both continuous and discrete time systems. Indeed, for manual tuning often the continuous time domain is used as in (1)–(2). For automated algorithms, as developed in Sec. 4 and Sec. 5, the discrete time domain is more natural. These domains can be directly linked, see [26][27].

In view of (2), G is decoupled in the relevant frequency ranges, in which case the elements e may be minimized step by step. This is investigated in the following subsections.

2.2.1 Traditional Feedforward Design Feedforward can effectively compensate for reference-induced error signals. In particular, f should be selected such that $r - Gf$ is minimized, possibly taking into account the weighting induced by the closed-loop system. In the low-frequency range, the system is decoupled and G_{flex} can be ignored in (2), in which case $f = G^{-1}r = s^2 r$, which is the Laplace transformation of the acceleration profile. Note that in (2), the mass of the rigid-body mode is normalized to unity. In practice, the feedforward signal is selected as $f = ms^2 r$, which is tuned in the time domain by decorrelating the measured error signal in (3) and the acceleration profile, details of which can be found in [28]. Furthermore, the compliance of the higher-order modes G_{flex} can be addressed in a snap term. Also, nonlinear effects such as friction can be effectively compensated. All these terms can be directly tuned manually in a straightforward manner [28].

2.2.2 Traditional Feedback Design For an appropriately designed feedforward signal, $\delta = r - Gf$ is small. In this case, the feedback controller has to minimize $S(\delta - v)$, where S is subject to a number of constraints and limitations [29], and hence cannot be made zero in general. The main idea is that rigid-body decoupling of G enables the shaping of the diagonal elements of S through a decentralized feedback controller [30, Sec. 10.6]. As a result, each diagonal element of K may be tuned independently. Typically, due to the low-frequency rigid-body behavior, a PID controller is tuned through manual loopshaping, followed by notch filters to account for the flexible modes in G_{flex} that hamper stability and/or performance.

2.2.3 Traditional Learning Control The feedforward controller in Sec. 2.2.1 performs well for a range of references r: the corresponding command signal f is automatically updated for each task, which possibly has a varying reference r. In the case where the setpoint r does not vary, see, e.g., [2] for an application example, the feedforward f may be obtained or improved using learning techniques. For SISO systems, these are fairly well-developed, see, e.g., [12][13] for an approach that relates to the design approach in Sec. 2.2.2.

2.2.4 Traditional Design Procedure Traditional motion control design divides the multivariable control design problems into subproblems that are manageable by manual control design. The traditional procedure consists of the following steps:

- identify an FRF of G_m, i.e., $G_m(\omega_i)$, for frequencies ω_i;
- decouple the plant to obtain an FRF of G;
- design K using manual loopshaping on the basis of the FRF, consisting of a PID with notches; and
- tune a feedforward controller, e.g., $f = m\ddot{r}$, using correlation techniques, optionally followed by learning control.

3. Precision Motion Control Developments

3.1 Future Mechatronic Designs A radically new lightweight mechatronic system design is envisaged to meet the requirements imposed by innovations in manufacturing machines and scientific instruments in terms of throughput, accuracy, and cost for the following reasons.

(1) Increased throughput is directly related to faster movements. The acceleration is directly determined by Newton's law $F = ma$. Here, the forces F that the actuators can deliver are bounded due to size and thermal aspects. Hence, throughput is increased by reducing the moving mass m.

(2) Increased accuracy is enabled by contactless motion, e.g., through magnetic levitation [31], since this avoids friction and enhances reproducibility. In addition, in certain applications, including EUV lithography [32][33], motion has to be performed in vacuum. Contactless motion is then essential to avoid pollution caused by mechanical wear and lubricants.

(3) Reduced cost can be enabled by reducing the requirements on material properties. In particular, present state-of-the-art systems involve exotic materials that provide high stiffness in conjunction with good thermal behavior.

Combining these aspects reveals that a lightweight system design is highly promising for next-generation motion systems. Such lightweight systems exhibit predominant flexible dynamical behavior, as is schematically illustrated in Fig. 4, as well as an increased susceptibility to disturbances [9, Sec. 9.5.2]. The prime reason why such systems are not yet feasible is the lack of control methodologies that handle the increased complexity, since the overall control design problem cannot be divided into subproblems as in Sec. 2, which are manageable by manual tuning techniques.

3.2 Challenges for Advanced Motion Control of Future Mechatronic Systems The envisaged mechatronic designs in Sec. 3.1 lead to several challenges for motion control design, including the following.

(1) Unmeasured performance variables are introduced by spatio-temporal deformations. In particular, the location where the performance is desired may not be directly measured. For example, performance in lithographic wafer stages is required at the spot of exposure, whereas sensors typically measure the edge of the stage, see Fig. 4. A key challenge lies in inferring the unmeasured performance variables. Similarly, in printing applications, both in 2D and 3D additive manufacturing, performance is desired where material is deposited on the substrate, while the sensor is mounted on the motor, with flexible dynamics in between, see Fig. 5.

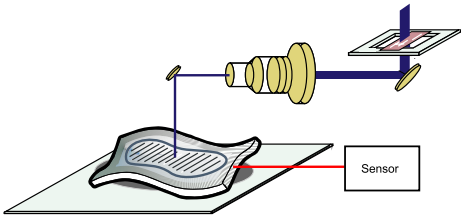

Fig. 4. Envisaged lightweight motion system in lithography. Top right: reticle stage containing reticle. Bottom left: envisaged lightweight wafer stage with spatio-temporal deformations due to flexible dynamics

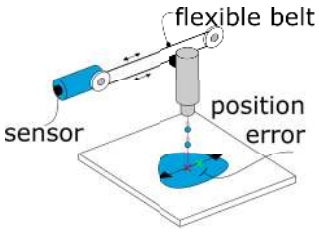

Fig. 5. Schematic illustration of a printing system where the performance variables are not directly measured. In particular, the sensor is mounted on the motor, while the belt deformation causes a deposition error

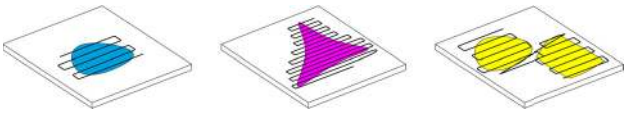

Fig. 6. Example of flexible tasks in 2D and 3D printing

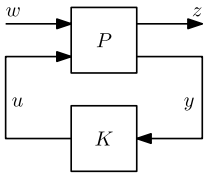

Fig. 7. Generalized plant setup, where $P(G)$. Note that K can be equal as in Fig. 3, but can also be extended to generate the signal f in Fig. 3

(2) Many additional inputs and outputs can be exploited to actively control the flexible dynamical behavior. In particular, the presence of spatio-temporal deformations and spatially distributed disturbances lead to highly complex deformations. A large number of sensors, which is enabled by the availability of inexpensive sensors and ubiquitous computing power, enable a high quality estimation of the dynamical behavior. Subsequently, spatially distributed actuators, including inexpensive smart materials such as piezos, will actively provide stiffness and damping to the mechanical deformations. Such an oversensed and/or overactuated situation is in sharp contrast to the present rigid-body situation, as is outlined in Sec. 2, and a key challenge lies in dealing with a large number of measured variables and manipulated variables.

(3) Position-dependent behavior is almost unavoidable in the case of spatio-temporal deformations, since motion systems perform motion by definition. For instance, for the single-mass system in Fig. 4, the spatio-temporal deformations are observed differently if the sensor is attached to the fixed world. In the sense of the model in (1), this implies that the c_i, b_i vectors depend on the actual position of the system, and (1) may be viewed as a local linearization of the overall nonlinear system. Similarly, in certain systems, including gantry stage designs, mass distributions change due to motion, leading to additional position-dependent behavior. A key challenge lies in handling the position dependence of future systems.

(4) A systems-of-systems perspective on motion control design provides a strong potential for performance enhancement of the overall system. In particular, typical manufacturing machines and scientific instruments involve multiple controlled subsystems, e.g., in the schematic illustration of a wafer scanner in Fig. 4, the wafer stage and reticle stage have to move relative to each other. In the design approach of Sec. 2, the overall goal is first divided into subsystems with a error budgets. As a result, performance limitations [29] in each subsystem will negatively impact the overall performance. A joint design enables that individual subsystems will be able to compensate each other's limitations. A main challenge lies in an increase of the complexity of the control problem.

(5) Thermal dynamics, in addition to mechanical deformations, are expected to become substantially more important due to increasing performance specifications, the use of less exotic materials for cost reduction, etc. A key challenge lies in the joint thermo-mechanical control design.

(6) Vibrations, including flow-induced vibrations of cooling liquids, floor vibrations, and immersion-hood in lithography, have to be attenuated. These increase proportionally to mass reduction [9, Sec. 9.5.2] and must be explicitly compensated.

(7) Versatile tasks are foreseen to become much more important in future manufacturing machines. For instance, (a) additive manufacturing allows for a large user-customization of products, (b) wafer scanners compensate for surface roughness [9, Sec. 9.4.1], (c) die bonders and wire bonders perform pick-and-place tasks based on actual product locations [2], and (d) 2D printing tasks involve varying references and media width [34]. As a result, the positioning systems in such machines have to perform a class of tasks, see Fig. 6.

3.3 A Generalized Plant Approach A generalized plant framework allows for a systematic way to address the future challenges in advanced motion control. In particular, the envisaged developments on future mechatronic system design, as described in Sec. 3.1, lead to challenges for motion control design, as are identified in Sec. 3.2.

The generalized plant is depicted in Fig. 7. The generalized plant is by no means new, and is at the basis of common optimization-based control algorithms [30]. However, the generalized plant allows a systematic and unified framework in which the challenges in Sec. 3.2 can be cast and conceptually addressed. In contrast, the traditional architecture in Fig. 3, which directly fits in the setup of Fig. 7, does not allow to address these challenges, even at a conceptual level.

In Fig. 7, z are the performance variables, addressing Challenge 1, which arises in addition to the already present measured variables y. Indeed, y and u are the measured variables and manipulated variables, respectively, the dimensions of which will drastically increase in view of Challenge 2. The variable w contains the exogenous inputs, typically including both reference signals and disturbances (Challenge 6), i.e., r and d in Fig. 3. Now, these variables may all be position-dependent (Challenge 3), and in addition, the variable r may vary for each task (Challenge 7). Furthermore, if multiple systems are addressed simultaneously, either due to their interaction, or their interaction due to a shared, overall machine control goal (Challenge 4), then this substantially increases the signal dimensions. Similarly, a joint thermal-mechanical control design (Challenge 5) involves signals and systems in both the thermal domain and the positioning domain.

The generalized plant approach in Fig. 7 directly reveals

the additional complexity arising from the challenges outlined in Sec. 3.2. Here $P(G)$ denotes the generalized plant, which contains the input-output plant G as well as the interconnection structure, e.g., Fig. 3. These increased complexity and accuracy requirements necessitate new developments in control algorithms, since these undermine the basic assumptions on which the approach in Sec. 2 relies. Indeed, the generalized plant is a conceptual framework to pose the overall problem, the actual design of motion controllers requires substantially more steps. Importantly, the controller K in Fig. 7 can be either a feedback controller, a feedforward controller, or both. Due to the fundamentally different objectives of these controllers, these are investigated sequentially in the forthcoming sections.

4. Feedback and Identification for Control

Feedback control, i.e., K in Fig. 3, is essential to deal with uncertainty in the system dynamics G and disturbances v. Indeed, the main goal of feedback is to render the system insensitive to such uncertainties. Note that the commonly imposed requirement of stability is only a direct consequence of the presence of uncertainties. In this section, feedback control design is investigated in view of the challenges in Sec. 3.2.

4.1 Norm-based Control In view of feedback, a model-based design is foreseen to be able to systematically address the challenges in Sec. 3.2. Here, model-based control refers to the use of parametric models using optimization algorithms [30]. For example, model-based optimal controller synthesis enables a systematic control design procedure for multivariable systems, enabling centralized controller structures. Also, a model-based design enables the estimation of unmeasured performance variables through the use of a model. It is emphasized that such a design is far from standard in industry, where the procedure in Sec. 2.2.2 is still most commonly used in state-of-the-art positioning systems.

To specify the control goal, the criterion

$$J(G,K) = \|\mathcal{F}_l(P(G),K)\| \cdots\cdots (4)$$

is posed, where the goal is to compute

$$K^{\text{opt}} = \arg\min_K J(G_o,K). \cdots\cdots (5)$$

Here, $\|.\|$ denotes a suitable norm, e.g., $\mathcal{H}_2$ or $\mathcal{H}_\infty$, and $\mathcal{F}_l$ denotes a lower linear fractional transformation (LFT), i.e.,

$$\mathcal{F}_l(G,K) = P_{11} + P_{12}K(I - P_{22}K)^{-1}P_{21}, \cdots\cdots (6)$$

where $P(G)$ is the interconnection structure and contains G. Indeed, $P(G)$ is the generalized plant depicted in Fig. 7 that encompasses most controller architectures, see [30, Sec. 3.8] for details. Next, note that $\mathcal{F}_l(G,K)$ is typically a closed-loop transfer function matrix, e.g., the general four-block problem

$$\mathcal{F}_l(G,K) = W\begin{bmatrix} G \\ I \end{bmatrix}(I+KG)^{-1}\begin{bmatrix} K & I \end{bmatrix}V, \cdots\cdots (7)$$

where W and V are user-chosen weighting filters of suitable dimensions. For instance, if $W = \begin{bmatrix} I & 0 \end{bmatrix}$, $V = \begin{bmatrix} 0 & I \end{bmatrix}^T$, then (7) reduces to

$$G(I+KG)^{-1}. \cdots\cdots (8)$$

It is emphasized that G_o in (5) denotes the true system, e.g., one of the systems depicted in Fig. 1. Note that G_o is unknown and will be represented by a model $\hat{G}$, as is elaborated next.

4.2 Nominal Modeling for Control: Motivation To arrive at a mathematically tractable optimization problem in (5), knowledge of the true system is represented through a model $\hat{G}$. The central question is how to obtain such a model that is suitable for controller design. System identification, or experimental modeling as opposed to first principles modeling, is an inexpensive, fast, and accurate approach to obtain such a model, see [35]–[37] for an overview. Indeed, the machine is often already built, enabling direct experimentation.

The model $\hat{G}$ that results from system identification is an approximation of the true system G_o for several reasons i) motion systems, typically of the form (2), often contain an infinite number of modes n_s, while a model of limited complexity may be desirable from a control perspective; ii) parasitic nonlinearities are present, including nonlinear damping [38]; and iii) identification experiments are based on finite time disturbed observations, leading to uncertainties on estimated parameters, e.g., ζ_i and ω_i in (2).

Although a large variety of system identification approaches and algorithms have been developed, many of these do not directly deliver a model that is suitable for designing a high-performance controller when implemented on the true system in view of (5). The main reason is that most identification techniques deliver a model that predicts the open-loop response as well as possible, instead of the desired closed-loop response, which is unknown before the controller is actually synthesized. This is illustrated in the following example.

Example 1 Consider the true system

$$G_o = \frac{1}{s^2} + \frac{1}{s^2 + 2\cdot 0.1\cdot(2\pi 100)s + (2\pi 100)^2} \cdots\cdots (9)$$

and the models

$$\hat{G}_1 = \frac{1}{s^2} - \frac{1}{s^2 + 2\cdot 0.1\cdot(2\pi 100)s + (2\pi 100)^2} \cdots (10)$$

and

$$\hat{G}_2 = \frac{1}{s^2 + 2\cdot 1s\cdot(2\pi 0.2) + (2\pi 0.2)^2} + \frac{1}{s^2 + 2\cdot 0.1\cdot(2\pi 100)s + (2\pi 100)^2}, \cdots\cdots (11)$$

see Fig. 8 for a Bode plot.

Next, an input

$$f(t) = \begin{cases} 1 & 0 \le t \le 0.1 \\ 0 & \text{elsewhere} \end{cases} \cdots\cdots (12)$$

is applied to the true system G_o as well as to both models $\hat{G}_1$ and $\hat{G}_2$, all of which are in open-loop, i.e., $K = 0$ in Fig. 3. In addition, r and v are zero in Fig. 3. The responses are depicted in Fig. 9. It is observed that $\hat{G}_1$ matches the true response accurately, while $\hat{G}_2$ shows a very different response. In particular, G_o and $\hat{G}_1$ show an unbounded response due to the rigid-body behavior, while $\hat{G}_2$ shows a bounded response. The Bode plots in Fig. 8 support this observation, since the model $\hat{G}_2$ does not have a -40 dB/dec slope at low frequencies. The key point is that most system identification techniques deliver a model that compares to $\hat{G}_1$, which is of course desired if the goal is to simulate G_o in open-loop as in Fig. 9.

Now, suppose that the optimal controller (5) is given by

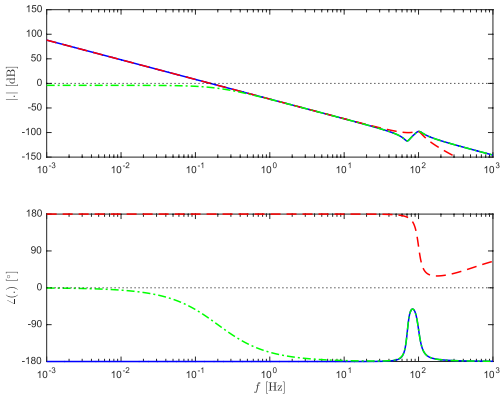

Fig. 8. Example 1: true system G_o in (9) (solid blue), model $\hat{G}_1$ in (10) (dashed red), model $\hat{G}_2$ in (11) (dash-dotted green)

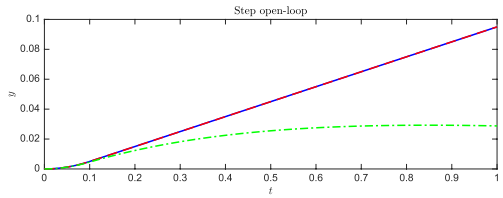

Fig. 9. Example 1: open-loop response to the input f in (12). True system G_o in (9) (solid blue). The model $\hat{G}_1$ in (10) (dashed red) closely matches the true output. However, model $\hat{G}_2$ in (11) (dash-dotted green) shows a strong deviation compared to the true response

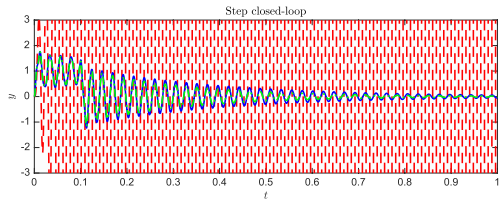

Fig. 10. Example 1: closed-loop response to the input f in (12) with optimal controller $K = 10^5$. True system G_o in (9) (solid blue). The model $\hat{G}_2$ in (11) (dash-dotted green) now closely matches the true output. In contrast, the model $\hat{G}_1$ in (10) (dashed red), which accurately predicted the open-loop response, performs poorly when predicting the closed-loop response

$K = 10^5$, i.e., a proportional controller to illustrate the main idea. When applying the same input (12), yet with $K = 10^5$ implemented as in Fig. 3, then the results in Fig. 10 are obtained. The difference of these closed-loop results are striking compared to Fig. 9: when the optimal controller $K = 10^5$ is implemented on the model $\hat{G}_1$, this does not even give a bounded response. In contrast, the model $\hat{G}_2$, that seemingly performed poorly in the *open-loop* response in Fig. 9, is very suitable for predicting the *closed-loop* response. □

The main conclusion from Example 1 is that the quality of models should be evaluated in view of their subsequent goal. The main goal of the models here is to deliver a controller that performs well on the true system in closed-loop. In this section, the identification of models in view of feedback control is investigated, the feedforward and ILC case is further elaborated on in Sec. 5.1.5.

4.3 Control-relevant Nominal Identification The quality of models depends on their goal. Here, the goal is given by (5). In particular, a model $\hat{G}$ is used to determine

$$K(\hat{G}) = \arg\min_K J(\hat{G}, K) \cdots\cdots\cdots\cdots\cdots\cdots\cdots (13)$$

which is then implemented on the true system G_o, leading to the achieved cost $J(G_o, K(\hat{G})$, which is bounded by

$$J(G_o, K^{\text{opt}}) \leq J(G_o, K(\hat{G})). \cdots\cdots\cdots\cdots\cdots\cdots (14)$$

The main question now is how to identify models that deliver a good controller in the sense that the bound (14) is tight. In addition, these models should preferably be of limited complexity, since the order of the controller is directly related to the order of the model $\hat{G}$. In contrast, in manually-tuned controllers, cf. Sec. 2.2.2, notch filters are only added for the modes in (1) that endanger stability and performance. Hence, the complexity of the model has to be justified by the control requirements.

A strategy to obtain such control-relevant models is to note that $J(G_o, K(\hat{G}))$ involves a norm. Hence, by rewriting and applying the triangle inequality for a certain K,

$$J(G_o, K) = J(\hat{G}, K) + J(G_o, K) - J(\hat{G}, K) \cdots\cdots (15)$$
$$\leq J(\hat{G}, K) + \|\mathcal{F}_l(P(G_o), K) - \mathcal{F}_l(P(\hat{G}), K)\|$$
$$\cdots\cdots\cdots\cdots\cdots (16)$$

Here, the first term $J(\hat{G}, K)$ can be minimized, which in fact equals the model-based design (13). The second term is a function of G_o, $\hat{G}$, and K. To arrive at a well-posed identification problem, assume that a reasonable feedback controller K^{exp} is already designed and implemented, e.g., following the procedure in Sec. 2.2.2. In fact, such a controller is typically required for identification experiments, since the open-loop system is often unstable, see (1). Then, $\mathcal{F}_l(P(G_o), K^{\text{exp}})$ is directly obtained as the (weighted) closed-loop system with K^{exp} implemented.

In this case, a suitable identification criterion is to substitute K^{exp} into the term in (16), leading to

$$\hat{G}_{CR} = \arg\min_{\hat{G}} \|\mathcal{F}_l(P(G_o), K^{\text{exp}}) - \mathcal{F}_l(P(\hat{G}), K^{\text{exp}})\|.$$
$$\cdots\cdots\cdots\cdots\cdots (17)$$

Essentially, in (17) a control-relevant model $\hat{G}_{CR}$ is identified that aims at representing *closed-loop* behavior. The minimization in (17) can be directly performed using the algorithm in, e.g., [39]. Note that (17) depends on the controller K. If K is chosen equal to K^{opt}, then typically the best result is obtained. Since K^{opt} is unknown, the result will depend on the quality of K^{exp}. To mitigate this dependence, the controller synthesis (13) and control-relevant identification (17) can be solved alternately, aiming to minimize the upper bound (16). Such an iterative procedure is at the basis of many approaches, including [40]–[45]. Unfortunately, such an iterative approach does not necessarily work, since the triangle inequality in (16) only holds valid for a fixed K, and does not allow for iterative updating of the controller. Still, (17) is a very valuable criterion for model identification, as will be shown in Sec. 4.5.

4.4 Toward Robust Motion Control The key reason why alternating between control-relevant identification (17) and model-based control design (13) does not work is the lack of robustness. Indeed, if $K(\hat{G})$ is designed solely based on $\hat{G}$, there is no reason to assume that it achieves a suitable level of performance on G_o. In fact, there are no guarantees that it actually stabilizes G_o in closed-loop. This motivates a robust control design, where the model quality is explicitly addressed during controller synthesis, as is outlined next.

In a robust control design [30], the true system behavior is represented by a model set $\mathcal{G}$ such that

$$G_o \in \mathcal{G}. \cdots\cdots (18)$$

Throughout, this model set is constructed by considering a perturbation around the nominal model $\hat{G}$, see Sec. 4.3, i.e.,

$$\mathcal{G} = \left\{ G \middle| G = \mathcal{F}_u(\hat{H}, \Delta_u), \Delta_u \in \mathbf{\Delta}_u \right\}, \cdots\cdots (19)$$

with the upper linear fractional transformation (LFT)

$$\mathcal{F}_u(\hat{H}, \Delta_u) = \hat{H}_{22} + \hat{H}_{21}\Delta_u(I - \hat{H}_{11}\Delta_u)^{-1}\hat{H}_{12} \cdots\cdots (20)$$

and $\hat{H}$ contains the nominal model $\hat{G}$ and the model uncertainty structure, see [30, (8.23)] for details. Note that $\hat{G}$ is recovered if the uncertainty is zero, so that $\hat{G} = \mathcal{F}_u(\hat{H}, 0)$.

It remains to specify Δ_u in more detail. In view of the considered motion control objectives, an $\mathcal{H}_\infty$ norm, i.e.,

$$\|H\|_\infty = \sup_\omega \bar{\sigma}(H(j\omega)), \cdots\cdots (21)$$

with $\bar{\sigma}$ denoting maximum singular value, is selected for the following reasons.

(1) $\mathcal{H}_\infty$-norm-bounded uncertainty enables a frequency-dependent characterization of dynamic uncertainty, which is very well suited for representing lightly damped modes in systems of the form (1). This is in sharp contrast to parameter uncertainty as is used in, e.g., [46].

(2) The $\mathcal{H}_\infty$ norm provides a suitable means to quantify performance objectives for motion systems in (4). In particular, the $\mathcal{H}_\infty$ norm allows a loopshaping-based design, see [47][48] for a general perspective and [7][49]–[52] for a motion control perspective. In addition, controller synthesis is typically most straightforward if a single norm is used for representing uncertainty and specifying the performance objectives.

Hence,

$$\mathbf{\Delta}_u = \left\{ \Delta_u \in \mathcal{H}_\infty \;\middle|\; \|\Delta_u\|_\infty \leq \gamma \right\}, \cdots\cdots (22)$$

where $\gamma \in \mathbb{R}_+$. Associated with $\mathcal{G}$ is the worst-case criterion

$$J_{\mathrm{WC}}(\mathcal{G}, K) = \sup_{G \in \mathcal{G}} J(G, K). \cdots\cdots (23)$$

Hence, by minimizing the worst-case performance

$$K^{\mathrm{RP}} = \arg\min_K J_{\mathrm{WC}}(G, K), \cdots\cdots (24)$$

the controller K^{RP} achieves robust performance in the sense that using (18), it leads to the tight upper bound

$$J(G_o, K^{\mathrm{RP}}) \leq J_{\mathrm{WC}}(\mathcal{G}, K^{\mathrm{RP}}). \cdots\cdots (25)$$

Hence, this leads to a performance guarantee when K^{RP} is implemented on the true system G_o. This is in sharp contrast to (14), which may actually be unbounded.

4.5 Modeling for Robust Motion Control Robust control provides a performance guarantee when implementing the controller K^{RP} on the true system G_o. The question on how to minimize the upper bound (25) hinges on the model set $\mathcal{G}$. Essentially, this involves the robust-control-relevant identification of a model set, which is the counterpart of the control-relevant identification problem of a nominal model $\hat{G}$ in Sec. 4.3.

The main idea is to follow a very similar approach as in Sec. 4.3. In particular, assume again that a controller K^{exp} is already implemented. Then, instead of minimizing (4) over K as in (24), it is minimized for the entire set $\mathcal{G}$, leading to the robust-control-relevant identification criterion

$$\mathcal{G}_{RCR} = \min_{\mathcal{G}} J_{\mathrm{WC}}(\mathcal{G}, K^{\mathrm{exp}}), \cdots\cdots (26)$$
$$\text{subject to (18).}$$

Combining the arguments implies that

$$J(G_o, K^{\mathrm{RP}}) \leq J_{\mathrm{WC}}(\mathcal{G}_{RCR}, K^{\mathrm{RP}}) \leq J_{\mathrm{WC}}(\mathcal{G}_{RCR}, K^{\mathrm{exp}}), \cdots\cdots (27)$$

hence guaranteed performance enhancement is achieved. Although this also depends on K^{exp}, it can be iterated, leading to monotonous performance enhancement [53], which is in sharp contrast to the suggested iterative procedure in Sec. 4.3.

The key question is how to actually determine the model set (26). The approach pursued here is to continue along the path in Sec. 4.3, i.e., to determine a control-relevant model as in (17). A second step aims at extending the model $\hat{G}_{CR}$ with $\mathbf{\Delta}_u$ such that (26) is actually addressed. Many techniques have been developed for selecting the structure of uncertainty, e.g., [54, Table 9.1], as well as quantifying its size [55][56]. However, the closed-loop aspect of the identified models, as in Example 1, has important consequences.

(1) Constraint (18) has to be satisfied for (25) to hold. Although this may seem trivially satisfied by increasing the size of $\mathbf{\Delta}_u$, note that typical uncertainty structures are based on open-loop reasoning. In particular, suppose that in Example 1
$$\mathcal{G} = \left\{ G \middle| G = \hat{G}_2 + \Delta_u, \|\Delta_u\|_\infty \leq \gamma \right\}. \cdots\cdots (28)$$
Then, since $\hat{G}_2 \in \mathcal{H}_\infty$ and by (28), $\mathcal{G} \subset \mathcal{H}_\infty$. However, since $G_o \notin \mathcal{H}_\infty$, (18) cannot be satisfied. The main reason is that G_o contains a rigid-body mode, which is neither included in $\hat{G}_2$, nor in an $\mathcal{H}_\infty$-norm-bounded perturbation Δ_u. This is confirmed by Fig. 8, where $\hat{G}_2$ has a bounded magnitude, yet $G_o \to \infty$ for $\omega \to 0$. Hence, no bounded Δ_u can capture the model mismatch using the structure (28).

(2) Suppose that the previous issue 1 is appropriately dealt with, and a certain bound γ guarantees that (18) is satisfied, the next question is how this actually minimizes $J_{\mathrm{WC}}(\mathcal{G}, K^{\mathrm{exp}})$ over $\mathcal{G}$ in (26). Indeed, often $\mathcal{G}$ satisfies (18), yet contains an element or a subset that is not stabilized by K^{exp}, in which case (26) is unbounded, see, e.g., [17, Table 1].

(3) Suppose that issue 1 and 2 are addressed, the final question is how $J_{\mathrm{WC}}(\mathcal{G}, K^{\mathrm{exp}})$ in (26) can be actually minimized.

These three issues are of crucial importance to avoid conservatism in the entire robust control design procedure. Indeed,

robust control is often experienced to lead to conservative results or may need a very large user-interaction, e.g., [51][57], due to inappropriately dealing with Issues 1 - 3, above.

The main trick to address Issues 1 and 2 has a very long history in control and is known as the dual form of the Youla parameterization. The Youla parameterization [58] parameterizes all controllers that stabilize a certain system. The dual form, as is considered here, see also [53][59]–[62], parameterizes all candidate systems that are closed-loop stable with K^{exp} implemented. In particular,

- the dual-Youla uncertainty structure is generated around the nominal model $\hat{G}$ obtained from Sec. 4.3,
- G_o is stabilized by K^{exp}, hence (18) is satisfied for a sufficiently large γ,
- all elements in $\mathcal{G}$ are stabilized, hence $J_{\text{WC}}(\mathcal{G}, K^{\text{exp}})$ in (26) remains bounded.

The remaining step to obtain a robust-control-relevant model set in the sense of (26) is to appropriately define the distance metric. Indeed, there is a large amount of freedom left in the dual-Youla parameterization. Recently, in [63], this freedom is exploited through a new coprime factorization, which directly connects the size of uncertainty γ in (22) and the control-relevant identification criterion (17). The underlying theory closely connects to recent developments in, e.g., [64]. A key consequence of this approach is that it provides an automatic scaling of the uncertainty, both in input/output directions and frequency. In turn, this enables the use of unstructured uncertainty in (22), which has important consequences for solving (24), e.g., using $D-K$ iterations [65].

4.6 Identification Procedure for Robust Motion Control Combining the developments in the preceding sections leads to the following design procedure.

(1) Specify a control objective J in (4) using the $\mathcal{H}_\infty$ norm, e.g., using loop-shaping design as in Sec. 2.2.2.

(2) Identify a nominal model $\hat{G}$ by minimizing (17) using data collected while K^{exp} is implemented.

(3) Extend the nominal model with the dual-Youla uncertainty structure as is outlined in Sec. 4.5, and determine the size of γ using any model uncertainty quantification procedure that delivers the minimal γ such that (18) is satisfied, e.g., [66]–[68].

(4) Compute and implement the optimal robust controller (24). If the performance is not satisfactory, repeat the procedure from Step 1.

The overall design procedure leads to nonconservative robust motion controllers and applies to highly complex systems. It enables new developments in motion control and addresses the challenges in Sec. 3.2 as is illustrated next.

4.7 Case Studies The procedure in Sec. 4.6 allows the design of advanced motion controllers that address the challenges in Sec. 3.2. These are elaborated next.

4.7.1 Case 1: Multivariable Modeling for Robust Control To show that the approach in Sec. 4.6 can deal with multivariable dynamics, a robust-control-relevant model set in the sense of (26) of the wafer stage in Fig. 1(a) is identified. The control goal in (4) is set to a bandwidth [30, Sec. 2.4.5] of 90 Hz with PID characteristics.

The identification results are depicted in Fig. 11. The model $\hat{G}$ is of order 8, corresponding to $n_{RB}=2$ and $n_s=2$ in (1). In addition, the uncertainty is tuned towards the control

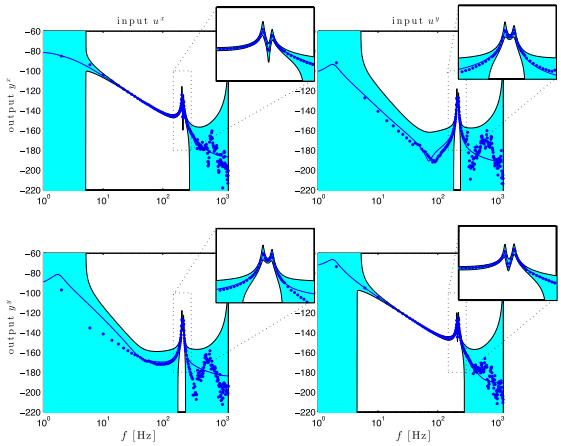

Fig. 11. Sec. 4.7.1: identified model set of the system in Fig. 1(a), with $\hat{G}$ (solid blue), $\mathcal{G}$ (cyan). Robust-control-relevance emphasizes the bandwidth region around 90 Hz, as well as the first two resonance phenomena [17]

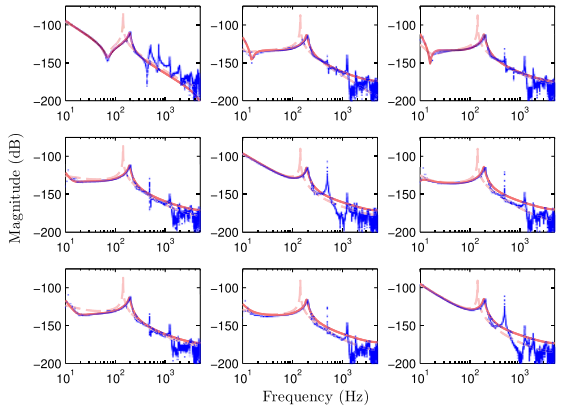

Fig. 12. Sec. 4.7.2: Overactuation of a prototype wafer stage [69]. The original model $\hat{G}$ has torsion mode with a resonance frequency of 143 Hz (dashed red). After closing the torsion loop, this resonance shifts to 193 Hz, where the equivalent plant model is shown (solid red). The identified frequency response function with the torsion loop closed (dotted blue) confirms the result

objective: the uncertainty is small in the bandwidth region and the first two resonances, which typically need notches in the traditional manual design procedure in Sec. 2.2.2. In addition, at low and high frequencies, a very large uncertainty is tolerated. The model set has been shown to lead to a factor two error reduction after 1 design cycle, see [17] for details. This error can be further reduced by repeating the design cycle in Sec. 4.6, as well as an error-based redesign [26].

4.7.2 Case 2: Overactuation The closed-loop bandwidth is often limited by resonance phenomena [69], even if multivariable loopshaping techniques [52] are used that address the input/output directionality of G_{flex} in (2). In view of the ideas in Sec. 3.2, additional actuators and sensors can be exploited. From a practical perspective, these can be employed to add active damping and stiffness. This technique has been successfully applied to a prototype wafer stage, where in the result of Fig. 12 a single actuator and sensor pair address the torsion mode, leading to a 35% bandwidth increase compared to the traditional input-output situation. These techniques are being extended to the 14 input-14 output prototype reticle

stage in Fig. 1(b), which can potentially achieve a significant accuracy and throughput enhancement by lightweight stage design, see Sec. 3.1. Finally, it is emphasized that the use of overactuation and oversensing has important benefits compared to traditional notch filters, as mentioned in Sec. 2.2.4. In particular, notch filters essentially render the vibrational modes unobservable, and only focus on local performance. In contrast, the proposed approach using overactuation and oversensing typically improves global performance [23].

4.7.3 Case 3: Inferential Control The procedure in Sec. 4.6 can be directly extended towards dealing with unmeasurable performance variables, in which case z contains variables that are not contained in y. The main idea is that a model is made that enables prediction of the unmeasurable performance variables, e.g., using temporary sensors. This requires an extension of the controller structure in Fig. 3, see [25] for details and an experimental example.

4.7.4 Case 4: Position-dependent Control Motion systems perform motions by definition. Hence, it can be expected that the system in Fig. 4 is position dependent, since the sensor observes the mode-shapes differently for changing positions. As a result, the position-dependence of the observation enables casting the system into the framework of linear parameter-varying (LPV) systems [70][71], for which reliable synthesis techniques are available. However, the identification of such systems from data is challenging [72]. Recently, a new approach has been developed [73] to model position-dependent systems for LPV control, which consists of two steps.

(1) Identify the system at a large number of frozen positions n_θ, which are considered as $n_y \cdot n_\theta$ auxiliary outputs. Identify the high-dimensional n_u input $n_y \cdot n_\theta$ output system using the procedure in Sec. 4.3 and Sec. 4.5.

(2) Interpolate the modeshapes to obtain a model with a continuous position dependence.

Experimental results are promising, see Fig. 13.

4.7.5 Case 5: Systems of Systems The overall control of the wafer stage in Fig. 4 involves several subsystems, including the wafer stage and the reticle stage. The overall control problem is the relative positioning of the wafer with respect to the reticle. Instead of dividing the overall control problem in independent subproblems, the overall framework of Fig. 7 enables the direct solution of the overall problem through the approach in Sec. 4.6. Interestingly, the theory developed in Sec. 4.4–Sec. 4.5 also allows for a systematic add-on, see [74] for recent results in this direction, as well as references therein.

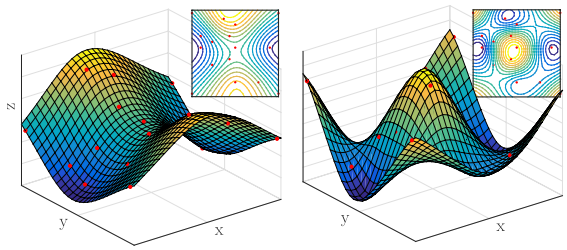

Fig. 13. Sec. 4.7.4: identification of position-dependent motion systems: 5th and 9th estimated mode of the prototype lightweight motion system of Sec. 4.7.2 [73]

4.7.6 Case 6: Thermomechanical Systems So far, the focus has mainly been on motion control. However, thermal aspects are becoming significant for increasing accuracy. These directly fit in the setup of Fig. 7, and the approach in Sec. 4.6 has recently been applied to a thermal control system with thermal actuators and sensors [75]. This also enables compensating for thermal deformations in motion control.

4.7.7 Case 7: Vibrations The presence of exogenous disturbances is essential and addressed in various aspects, including the use of active vibration isolation systems (AVIS) [66][76], compensation through disturbance observers [77], and disturbance-based control [26][78].

4.8 Discussion and Overall Design Procedure In Sec. 4.7, several successful case studies of the approach in Sec. 4.6 are presented. This raises the question whether the approach in Sec. 4.6 has disadvantages compared to the traditional approach in Sec. 2.2.2. Although the theory is laid out, the algorithms still require significant user interaction. Also, numerical aspects are highly challenging [79]–[82], especially for the complex systems envisaged in Sec. 3.2.

Taking into account the current level of maturity of the tools described in this section and based on significant experience with multivariable motion systems, the following procedure enables a systematic design of motion controllers.

Procedure 1 Advanced motion control design procedure.

1. Interaction analysis. Decoupled?
   - yes: independent SISO design (Sec. 2.2.2). No: next step
2. Static decoupling (Equation (2)). Decoupled?
   - yes: independent SISO design (Sec. 2.2.2). No: next step
3. Decentralized MIMO design: loop closing procedures [83, Sec. 1.3.3]
   - robustness for interaction, e.g., using factorized Nyquist
   - design for interaction, e.g., sequential loop closing

   Not successful? Next step
4. Optimal & robust control (Sec. 4.6)
   - centralized controller with typically best performance
   - requires parametric model

Procedure 1 has proven to perfectly balance effort vs. control requirements [83]. Indeed, the effort in terms of user intervention and modeling are only increased if necessitated by the control requirements. Interestingly, the first three steps are all based on FRF data, whereas the last step, i.e., the procedure of Sec. 4.6 involves the use of a parametric model.

Note that all four steps in Procedure 1 are based on FRF data. Indeed, Step 4 in Procedure 1 involves the identification problem Sec. 4.3, which is again based on FRFs. This has led to a renewed interest in identifying FRFs of complex mechatronic systems, where traditionally noise excitation has been used [7][51]. These have been extended towards periodic excitation for motion systems [17], and more recently substantial advancements have been made using local parametric modeling techniques [84], including extensions to linear parameter-varying (LPV) systems [85] and multivariable systems [86].

5. Feedforward and Learning

Feedforward and learning control are essential for high performance motion control. In this section, first learning control is investigated, the connection to feedforward is further outlined in Sec. 5.1.5.

5.1 Learning and Repetitive Control Iterative learning control (ILC) [13] is particularly promising for posi-

tioning systems that perform repeating tasks. Typically, the feedforward signal f in Fig. 3 is updated based on past experiments or trials j, e.g.,

$$f_{j+1} = Q(f_j + Le_j), \quad (29)$$

with Q and L appropriate learning filters. Essentially, (29) involves a trial-domain feedback, hence the resulting system is a 2D system [87]. For SISO systems, a well-developed design framework is available [12], yet in view of the challenges in Sec. 3.2, ILC algorithms of the form (29) are not directly applicable. The challenges in Sec. 3.2 are now briefly investigated in the context of ILC, see [19] for a more detailed overview. Repetitive control [88][89] is a control strategy that is similar to ILC, yet does not reset the system after each repetition. The mentioned challenges are focussed on ILC, yet also apply to repetitive control situations.

5.1.1 Inferential ILC for Unmeasurable Feedback Signals Often, the performance variables are not directly accessible to the feedback controller, but they can be measured *after* a task is completed. For instance, in printing invisible markers can be used [90, Sec. 5.3]. This idea is illustrated in Fig. 14. When ILC is applied to the z measurement, whereas feedback is applied to y, it is generally impossible to track a reference for both, i.e., to ensure that both $r - y$ and $r - z$ are small. This can lead to severe consequences when attempting to do so, e.g., using integral action in conjunction with ILC,

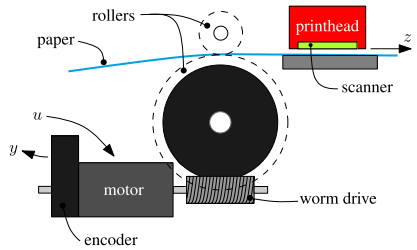

Fig. 14. Schematic side-view illustration of the positioning drive in a printer system for inferential ILC in Sec. 5.1.1. The paper position z is controlled using the motor. The feedback uses real-time encoder measurements y. The performance z is measured line-by-line using the scanner, which is used for iterative learning control purposes

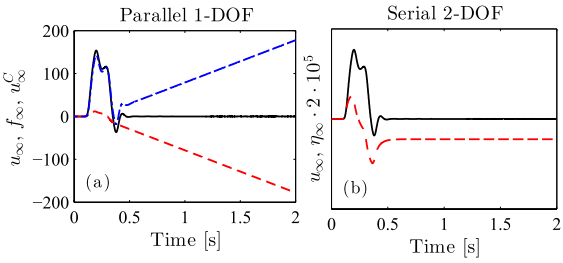

Fig. 15. Signals after convergence of inferential ILC in Sec. 5.1.1. In traditional motion control architectures (Fig. 3), the ILC command signal f (red dashed) cancels the feedback controller output (blue dashed, also Ke in Fig. 3), leading to an internally unstable system (the overall input u (black solid) remains bounded). An adapted controller architecture leads to closed-loop stability in a 2D systems setting, see [91], leading to both a bounded ILC command signal f (black solid) and bounded feedback controller output (red-dashed)

as is illustrated in Fig. 15. To systematically address these aspects, a 2D systems approach, see [87], is used in the context of inferential ILC framework developed in [91], which also encompasses related inferential ILC approaches, including [92].

5.1.2 Multivariable ILC with Additional Inputs and Outputs ILC for multivariable systems is significantly more challenging compared to feedback. Although ILC is fairly robust with respect to modeling errors, it is effective up to the Nyquist frequency, imposing model quality requirements over the entire frequency range, which is in sharp contrast to the results in Fig. 11. In [93], the ILC analogue of Procedure 1, which aims at advanced motion feedback control design, is developed. Indeed, as is shown in Fig. 16, a decentralized ILC that ignores interaction may lead to an unstable ILC algorithm in the iteration domain when both loops are closed simultaneously. In Fig. 17, several solutions are shown that lead to a stable ILC iteration. Here, the decentralized design requires the least modeling effort, i.e., only the diagonal terms need to be modeled parametrically. A centralized design typically improves the performance, yet requires a full multivariable parametric model. Hence, the procedure in [93] appropriately balances the required modeling effort and the performance requirements. As an additional aspect in dealing with multivariable systems, the potential of additional inputs for ILC is established in [94].

5.1.3 ILC for Position-dependent Systems Since ILC is effective over a much larger frequency range compared to feedback, the effect of position-dependent dynamics is amplified. In particular, when applying ILC to the position-dependent printer in Fig. 1(d), linearized models either lead to a divergent scheme or slow convergence, see Fig. 18. An LTV approach, see [95], can effectively deal with position-dependent behavior. Initial results towards an LPV approach are reported in [96], whereas an LPTV approach is pursued in [97].

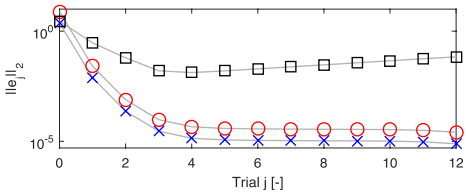

Fig. 16. Multivariable ILC in Sec. 5.1.2. Independently designed ILC loops (○, ×) converge when implemented independently. However, when implemented simultaneously (□), the multivariable ILC does not converge

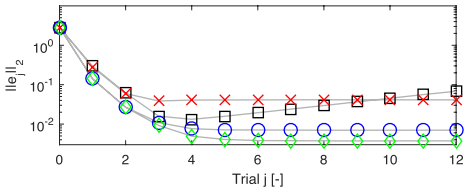

Fig. 17. Multivariable ILC in Sec. 5.1.2. Multivariable ILC designs [93]: decentralized with robustness for interaction (×), centralized based on $\mathcal{H}_\infty$ preview control (◇), and centralized based on MIMO ZPETC (○) lead to convergent ILC algorithms. In contrast, a decentralized design that ignores interaction (□) leads to a divergent error norm

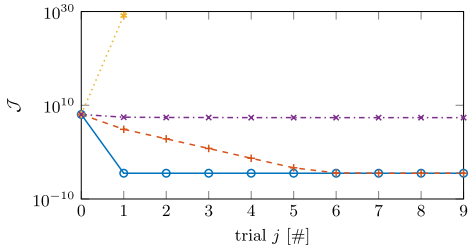

Fig. 18. Position-dependent ILC in Sec. 5.1.3. Applying ILC to the position-dependent printer in Fig. 1(d). First, a linearized model at an edge position is used. This LTI model leads to a divergent iteration when applied to the position-dependent system (∗). Inclusion of a Q-filter for robustness leads to convergence, yet limited performance enhancement (×). Linearization of the model at a different location leads to a convergent ILC (+) without the need for a Q-filter, hence leading to improved performance. An LTV design [95] leads to superior performance: it achieves high performance and fast convergence

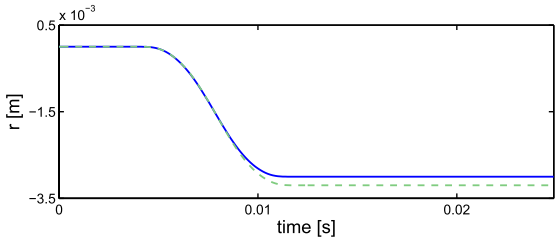

Fig. 19. Varying references in ILC, see Sec. 5.1.5, as occurring in the wire bonder of Fig. 1(c). Due to varying product locations, the end-position varies

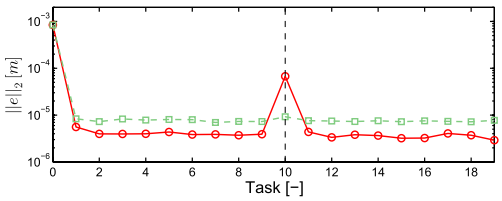

Fig. 20. Varying references in ILC, see Sec. 5.1.5, as occurring in the wire bonder of Fig. 1(c). In iteration 0 – 9, the blue reference of Fig. 19 is used, while from iteration 10 at further, the green dashed reference of Fig. 19 is used. Clearly, standard ILC (red) is highly sensitive to reference changes, whereas the proposed ILC with basis function in [2] (green) enables high performance for versatile references

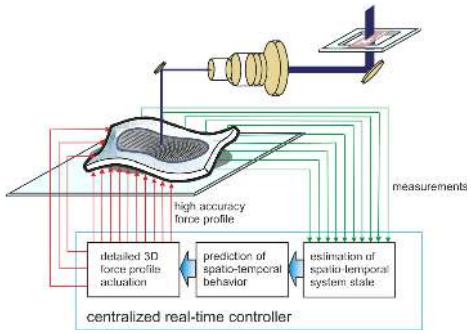

Fig. 21. Control of future lightweight stages as in Fig. 4. Based on measured sensor information, the controller predicts the spatio-temporal behavior (either locally at the performance location or globally), and determines a suitable force profile for accurately positioning the stage and its internal flexible dynamics

5.1.4 Systems of Systems The design procedure in [93] can directly be applied to such systems, whereas a systematic ILC add-on as in Sec. 4.7.5 is developed in [98].

5.1.5 Flexible Tasks One of the largest drawbacks of traditional ILC is that it requires the reference r in Fig. 3 to be fixed. This is in sharp contrast to traditional feedforward control as is outlined in Sec. 2.2.1. The main goal of recent research, including [90][99]–[101] has been to combine the performance advantages of learning control with the extrapolation capabilities of the feedforward structures in Sec. 2.2.1.

As an application example, the wire bonder in Fig. 1(c) has varying references for every product due to position variability. As a result, the end-position of the point-to-point motion varies, see Fig. 19. ILC is highly susceptible to such changes, see Fig. 20, since a reference change at iteration 10 leads to a large performance degradation. Note that the reference is kept constant from iteration 0–9 for illustration purposes only. For more details on the wire bonder application, see [2]. For a successful applications on the printer system of Fig. 1(d), see [34]. For an application to the wafer stage of Fig. 1(a), see [102].

The theoretical framework is further extended towards input shaping [103] and rational feedforward structures in [104]–[106], which have as key advantage that these can *exactly* compensate non-minimum phase dynamics, see [107] for a detailed exposition, and also [95][108][109] for further details and applications.

Finally, a strongly related approach that further connects to system identification in Sec. 4.3 is developed in [28][110][111]. In particular, this approach essentially constitutes a framework for identification of models for feedforward, where the answer lies in identifying the inverse system directly using instrumental variable system identification [112]. For a detailed comparison to ILC-based approaches, see [102]. Notice that in ILC, the identification criterion for the model, which is needed to construct the learning filter, is slightly different and should be chosen such that the model error is less than 100% in the relevant frequency range of interest, see [93] for details in this direction.

6. Outlook

Advanced motion control is a highly challenging and important area. Several issues arising from ongoing developments in applications have been identified, along with several solution strategies that are being developed. Many related challenges, e.g., for specific application areas, have not been addressed in the present paper, including [4][113]–[116]. In addition, numerical aspects are highly challenging for complex systems, in control [117], system identification [79]–[82], and learning [95]. In addition, resource-efficient approaches for ILC based on sparse optimization are investigated in [118]. Furthermore, nonlinear control techniques have been investigated in, e.g., [119]–[121]. Digital implementation aspects are investigated in [116][122][123]. Finally, data-driven techniques to avoid modeling altogether are being investigated in, e.g., [121][124][125] for feedback control and [126][127] for ILC.

In the near future, developments in advanced motion control may enable a paradigm shift in mechatronic system

design. Indeed, a very lightweight design is foreseen, see Fig. 4, where stiffness is obtained through active control. Indeed, based on measured sensor information, the controller predicts the spatio-temporal behavior (either locally at the performance location or globally, and determines a suitable force profile for accurately positioning the stage and its internal flexible dynamics, see Fig. 21 for details. In addition, thermal behavior will be actively controlled. These future systems may achieve unprecedented accuracy, speed, and cost, and will communicate with other subsystems to increase overall system performance.

Acknowledgment

I would like to thank many collaborators over the past decade, both in academia and industry, and in particular Lennart Blanken, Frank Boeren, Joost Bolder, Enzo Evers, Egon Geerardyn, Robbert van Herpen, Robin de Rozario, Robbert Voorhoeve, and Jurgen van Zundert, as well as Maarten Steinbuch and Okko Bosgra, for the joint research that led to the results in this paper.

References

(1) V.M. Martinez and T.F. Edgar: "Control of lithography in semiconductor manufacturing", *IEEE Contr. Syst. Mag.*, Vol.26, No.6, pp.46–55 (2006)
(2) F. Boeren, A. Bareja, T. Kok, and T. Oomen: "Frequency-domain ILC approach for repeating and varying tasks: With application to semiconductor bonding equipment", *IEEE Trans. Mech.*, Vol.21, No.6, pp.2716–2727 (2016)
(3) D. Abramovitch, S. Andersson, L. Pao, and G. Schitter: "A tutorial on the mechanics, dynamics, and control of atomic force microscopes", In Proc. 2007 Americ. Contr. Conf. pp.3488–3502, New York, NY, USA (2007)
(4) R. Findeisen, M.A. Grover, C. Wagner, M. Maiworm, R. Temirov, F.S. Tautz, M.V. Salapaka, S. Salapaka, R.D. Braatz, and S.O.R. Moheimani: "Control on a molecular scale: a perspective", In Proc. 2016 Americ. Contr. Conf., pp.3069–3076, Boston, MA, USA (2016)
(5) K. Ohnishi, M. Shibata, and T. Murakami: "Motion control for advanced mechatronics", *IEEE Trans. Mech.*, Vol.1, No.1, pp.56–67 (1996)
(6) H.S. Lee and M. Tomizuka: "Robust motion controller design for high-accuracy positioning systems", *IEEE Trans. Ind. Electr.*, Vol.43, No.1, pp.48–55 (1996)
(7) M. Steinbuch and M.L. Norg: "Advanced motion control: An industrial perspective", *Eur. J. Contr.*, Vol.4, No.4, pp.278–293 (1998)
(8) J. Stoev, J. Ertveldt, T. Oomen, and J. Schoukens: "Tensor methods for MIMO decoupling and control design using frequency response functions", *Mechatronics*, Vol.45, pp.71–81 (2017)
(9) R. Munnig Schmidt, G. Schitter, and J. van Eijk: "The Design of High Performance Mechatronics", Delft University Press, Delft, The Netherlands (2011)
(10) A.J. Fleming and K.K. Leang: "Design, Modeling and Control of Nanopositioning Systems", Springer (2014)
(11) H. Butler: "Position control in lithographic equipment an enabler for current-day chip manufacturing", *IEEE Contr. Syst. Mag.*, Vol.31, No.5, pp.28–47 (2011)
(12) M. Steinbuch and R.v.d. Molengraft: "Iterative learning control of industrial motion systems", In 1st IFAC Symp, Mech. Syst., pp.967–972, Darmstadt, Germany (2000)
(13) D.A. Bristow, M. Tharayil, and A.G. Alleyne: "A survey of iterative learning control: A learning-based method for high-performance tracking control", *IEEE Contr. Syst. Mag.*, Vol.26, No.3, pp.96–114 (2006)
(14) G.J. Balas and J.C. Doyle: "Control of lightly damped, flexible modes in the controller crossover region", *J. Guid., Contr., Dyn.*, Vol.17, No.2, pp.370–377 (1994)
(15) D. Hyland, J. Junkins, and R. Longman: "Active control technology for large space structures", *J. Guid., Contr., Dyn.*, Vol.16, No.5, pp.801–821 (1993)
(16) I.R. Petersen and A. Lanzon: "Feedback control of negative-imaginary systems", *IEEE Contr. Syst. Mag.*, Vol.30, No.5, pp.54–72 (2010)
(17) T. Oomen, R. van Herpen, S. Quist, M. van de Wal, O. Bosgra, and M. Steinbuch: "Connecting system identification and robust control for next-generation motion control of a wafer stage", *IEEE Trans. Contr. Syst. Techn.*, Vol.22, No.1, pp.102–118 (2014)
(18) T. Oomen: "Advanced motion control for next-generation precision mechatronics: Challenges for control, identification, and learning", In IEEJ International Workshop on Sensing, Actuation, Motion Control, and Optimization (SAMCON), pp.1–12, Nagaoka, Japan (2017)
(19) L. Blanken, R. de Rozario, J. van Zundert, S. Koekebakker, M. Steinbuch, and T. Oomen: "Advanced feedforward and learning control for mechatronic systems", In Proc. 3rd DSPE Conf. Prec. Mech., pp.79–86, Sint-Michielsgestel, The Netherlands (2016)
(20) A.J. Fleming: "Measuring and predicting resolution in nanopositioning systems", *Mechatronics*, Vol.24, No.6, pp.605–618 (2014)
(21) W.K. Gawronski: Advanced Structural Dynamics and Active Control of Structures, Springer, New York, NY, USA (2004)
(22) A. Preumont: Vibration Control of Active Structures: An Introduction, volume 96 of Solid Mechanics and Its Applications, Kluwer Academic Publishers, New York, NY, USA, second edition (2004)
(23) S. Moheimani, D. Halim, and A.J. Fleming: Spatial Control of Vibration: Theory and Experiments, World Scientific, Singapore (2003)
(24) P.C. Hughes: "Space structure vibration modes: How many exist? Which ones are important?", *IEEE Contr. Syst. Mag.*, Vol.7, No.1, pp.22–28 (1987)
(25) T. Oomen, E. Grassens, and F. Hendriks: "Inferential motion control: An identification and robust control framework for unmeasured performance variables", *IEEE Trans. Contr. Syst. Techn.*, Vol.23, No.4, pp.1602–1610 (2015)
(26) T. Oomen, M. van de Wal, and O. Bosgra: "Design framework for high-performance optimal sampled-data control with application to a wafer stage", *Int. J. Contr.*, Vol.80, No.6, pp.919–934 (2007)
(27) T. Oomen: "Controlling aliased dynamics in motion systems? An identification for sampled-data control approach", *Int. J. Contr.*, Vol.87, No.7, pp.1406–1422 (2014)
(28) F. Boeren, T. Oomen, and M. Steinbuch: "Iterative motion feedforward tuning: a data-driven approach based on instrumental variable identification", *Contr. Eng. Prac.*, Vol.37, pp.11–19 (2015)
(29) M.M. Seron, J.H. Braslavsky, and G.C. Goodwin: Fundamental Limitations in Filtering and Control, Springer-Verlag, London, UK (1997)
(30) S. Skogestad and I. Postlethwaite: "Multivariable Feedback Control: Analysis and Design", John Wiley & Sons, West Sussex, UK, second edition (2005)
(31) J.C. Compter: "Electro-dynamic planar motor", *Prec. Eng.*, Vol.28, No.2, pp.171–180 (2004)
(32) G.D. Hutcheson: "The first nanochips", *Scient. Americ.*, pp.48–55, April (2004)
(33) B. Arnold: "Shrinking possibilities", *IEEE Spectrum*, Vol.46, No.4, pp.26–28, 50–56 (2009)
(34) J. Bolder, J. van Zundert, S. Koekebakker, and T. Oomen: "Enhancing flatbed printer accuracy and throughput: Optimal rational feedforward controller tuning via iterative learning control", *IEEE Trans. Ind. Electr.*, Vol.64, No.5, pp.4207–4216 (2017)
(35) L. Ljung: System Identification: Theory for the User, Prentice Hall, Upper Saddle River, NJ, USA, second edition (1999)
(36) R. Pintelon and J. Schoukens: System Identification: A Frequency Domain Approach, IEEE Press, New York, NY, USA, second edition (2012)
(37) H. Hjalmarsson: "From experiment design to closed-loop control", *Automatica*, Vol.41, pp.393–438 (2005)
(38) R.S. Smith: "Closed-loop identification of flexible structures: An experimental example", *J. Guid., Contr., Dyn.*, Vol.21, No.3, pp.435–440 (1998)
(39) T. Oomen and M. Steinbuch: "Identification for robust control of complex systems: Algorithm and motion application", In M. Lovera, editor, *Control-oriented modelling and identification: theory and applications*, IET (2015)
(40) R.J.P. Schrama: "Accurate identification for control: The necessity of an iterative scheme", *IEEE Trans. Automat. Contr.*, Vol.37, No.7, pp.991–994 (1992)
(41) M. Gevers: Towards a joint design of identification and control ? In H.L. Trentelman and J.C. Willems, editors, *Essays on Control: Perspectives in the Theory and its Applications*, chapter 5, pp.111–151, Birkhäuser, Boston, MA, USA (1993)
(42) R.A. de Callafon and P.M.J. Van den Hof: "Filtering and parametrization issues in feedback relevant identification based on fractional model representations", In Proc. 3rd Eur. Contr. Conf., pp.441–446, Rome, Italy (1995)
(43) P.M.J. Van den Hof and R.J.P. Schrama: "Identification and control - closed-loop issues", *Automatica*, Vol.31, No.12, pp.1751–1770 (1995)
(44) P.M.J. Van den Hof: "Closed-loop issues in system identification", *Annual Reviews in Control*, Vol.22, pp.173–186 (1998)
(45) P. Albertos and A. Sala: Multivariable Control Systems: An Engineering Approach, Springer-Verlag, London, UK (2004)
(46) M. Gevers, X. Bombois, B. Codrons, G. Scorletti, and B.D.O. Anderson: "Model validation for control and controller validation in a prediction error identification framework—part I: Theory", *Automatica*, Vol.39, No.3,

pp.403–415 (2003)
(47) D.C. McFarlane and K. Glover: *Robust Controller Design Using Normalized Coprime Factor Plant Descriptions*, vol.138 of *LNCIS*. Springer-Verlag, Berlin, Germany (1990)
(48) J.C. Doyle and G. Stein: "Multivariable feedback design: Concepts for a classical/modern synthesis", *IEEE Trans. Automat. Contr.*, Vol.26, No.1, pp.4–16 (1981)
(49) M. Steinbuch and M.L. Norg: "Industrial perspective on robust control: Application to storage systems", *Annual Reviews in Control*, Vol.22, pp.47–58 (1998)
(50) U. Schönhoff and R. Nordmann: "A $\mathcal{H}_\infty$-weighting scheme for PID-like motion control", In Proc. 2002 Conf. Contr. Appl., pp.192–197, Glasgow, Scotland (2002)
(51) M. van de Wal, G. van Baars, F. Sperling, and O. Bosgra: "Multivariable $\mathcal{H}_\infty/\mu$ feedback control design for high-precision wafer stage motion", *Contr. Eng. Prac.*, Vol.10, No.7, pp.739–755 (2002)
(52) F. Boeren, R. van Herpen, T. Oomen, M. van de Wal, and M. Steinbuch: "Non-diagonal $\mathcal{H}_\infty$ weighting function design: Exploiting spatial-temporal deformations for precision motion control", *Contr. Eng. Prac.*, Vol.35, pp.35–42 (2015)
(53) R.A. de Callafon and P.M.J. Van den Hof: "Suboptimal feedback control by a scheme of iterative identification and control design", *Math. Mod. Syst.*, Vol.3, No.1, pp.77–101 (1997)
(54) K. Zhou, J.C. Doyle, and K. Glover: Robust and Optimal Control, Prentice Hall, Upper Saddle River, NJ, USA (1996)
(55) W. Reinelt, A. Garulli, and L. Ljung: "Comparing different approaches to model error modeling in robust identification", *Automatica*, Vol.38, No.5, pp.787–803 (2002)
(56) J. Chen and G. Gu: Control-Oriented System Identification: An $\mathcal{H}_\infty$ Approach, John Wiley & Sons, New York, NY, USA (2000)
(57) R.A. de Callafon and P.M.J. Van den Hof: "Multivariable feedback relevant system identification of a wafer stepper system", *IEEE Trans. Contr. Syst. Techn.*, Vol.9, No.2, pp.381–390 (2001)
(58) B.D.O. Anderson: "From Youla-Kucera to identification, adaptive and nonlinear control", *Automatica*, Vol.34, No.12, pp.1485–1506 (1998)
(59) C. C.H. Ma: Comments on "A necessary and sufficient condition for stability of a perturbed system", *IEEE Trans. Automat. Contr.*, Vol.33, No.8, pp.796–797 (1988)
(60) F. Hansen, G. Franklin, and R. Kosut: "Closed-loop identification via the fractional representation: Experiment design", In Proc. 8th Americ. Contr. Conf., pp.1422–1427, Pittsburgh, PA, USA (1989)
(61) H. Niemann: "Dual Youla parameterisation", *IEE Proc.-Control Theory Appl.*, Vol.150, No.5, pp.493–497 (2003)
(62) S.G. Douma and P.M.J. Van den Hof: "Relations between uncertainty structures in identification for robust control", *Automatica*, Vol.41, No.3, pp.439–457 (2005)
(63) T. Oomen and O. Bosgra: "System identification for achieving robust performance", *Automatica*, Vol.48, No.9, pp.1975–1987 (2012)
(64) A. Lanzon and G. Papageorgiou: "Distance measures for uncertain linear systems: A general theory", *IEEE Trans. Automat. Contr.*, Vol.54, No.7, pp.1532–1547 (2009)
(65) A. Packard and J. Doyle: "The complex structured singular value", *Automatica*, Vol.29, No.1, pp.71–109 (1993)
(66) T. Oomen, R. van der Maas, C.R. Rojas, and H. Hjalmarsson: "Iterative data-driven $\mathcal{H}_\infty$ norm estimation of multivariable systems with application to robust active vibration isolation", *IEEE Trans. Contr. Syst. Techn.*, Vol.22, No.6, pp.2247–2260 (2014)
(67) E. Geerardyn, T. Oomen, and J. Schoukens: "Enhancing $\mathcal{H}_\infty$ norm estimation using local LPM/LRM modeling: Applied to an AVIS", In IFAC 19th Triennial World Congress, pp.10856–10861, Cape Town, South Africa (2014)
(68) T. Oomen and O. Bosgra: "Well-posed model uncertainty estimation by design of validation experiments", In 15th IFAC Symp. Sys. Id., pp.1199–1204, Saint-Malo, France (2009)
(69) R. van Herpen, T. Oomen, E. Kikken, M. van de Wal, W. Aangenent, and M. Steinbuch: "Exploiting additional actuators and sensors for nano-positioning robust motion control", *Mechatronics*, Vol.24, No.6, pp.619–631 (2014)
(70) M. Groot Wassink, M. van de Wal, C. Scherer, and O. Bosgra: "LPV control for a wafer stage: Beyond the theoretical solution", *Contr. Eng. Prac.*, Vol.13, pp.231–245 (2003)
(71) J. De Caigny, J.F. Camino, and J. Swevers: Interpolation-based modeling of MIMO LPV systems", *IEEE Trans. Contr. Syst. Techn.*, Vol.19, No.1, pp.46–63 (2011)
(72) P. Lopes des Santos, A. Perdicoúlis, C. Novara, J.A. Ramos, and D.E. Rivera, editors: *Linear Parameter-Varying System Identification: New Developments and Trends*, World Scientific (2011)
(73) R. de Rozario, R. Voorhoeve, W. Aangenent, and T. Oomen: "Spatio-temporal identification of mechanical systems: With application to global feedforward control of an industrial wafer stage", In IFAC 2017 Triennial World Congress, pp.15140–15145, Toulouse, France (2017)
(74) E. Evers, M. van de Wal, and T. Oomen: "Synchronizing decentralized control loops for overall performance enhancement: A Youla framework applied to a wafer scanner", In IFAC 2017 Triennial World Congress, pp.11332–11337, Toulouse, France (2017)
(75) J. Guo: "Positioning performance enhancement via identification and control of thermal dynamics: A MIMO wafer table case study", Master's thesis, Eindhoven University of Technology (2014)
(76) M. Boerlage, B. de Jager, and M. Steinbuch: "Control relevant blind identification of disturbances with application to a multivariable active vibration isolation platform", *IEEE Trans. Contr. Syst. Techn.*, Vol.18, No.2, pp.393–404 (2010)
(77) R. Voorhoeve, N. Dirkx, T. Melief, W. Aangenent, and T. Oomen: "Estimating structural deformations for inferential control: A disturbance observer approach", In 7th IFAC Symposium on Mechatronic Systems & 1st Mechatronics Forum International Conference, pp.642–648, Loughborough, UK (2016)
(78) J. van Zundert and T. Oomen: "On optimal feedforward and ILC: The role of feedback for optimal performance and inferential control", In IFAC 2017 Triennial World Congress, pp.6267–6272, Toulouse, France (2017)
(79) A. Bultheel, M. van Barel, Y. Rolain, and R. Pintelon: "Numerically robust transfer function modeling from noisy frequency domain data", *IEEE Trans. Automat. Contr.*, Vol.50, No.11, pp.1835–1839 (2005)
(80) R. van Herpen, T. Oomen, and M. Steinbuch: "Optimally conditioned instrumental variable approach for frequency-domain system identification", *Automatica*, Vol.50, No.9, pp.2281–2293 (2014)
(81) R. van Herpen, O. Bosgra, and T. Oomen: "Bi-orthonormal polynomial basis function framework with applications in system identification", *IEEE Trans. Automat. Contr.*, Vol.61, No.11, pp.3285–3300 (2016)
(82) R. Voorhoeve, A. van Rietschoten, E. Geerardyn, and T. Oomen: "Identification of high-tech motion systems: An active vibration isolation benchmark", In 17th IFAC Symp. Sys. Id., pp.1250–1255, Beijing, China (2015)
(83) T. Oomen and M. Steinbuch: "Model-based control for high-tech mechatronic systems", In The Handbook on Electrical Engineering Technology and Systems, Volume 5 – Factory and Industrial Automated Systems, CRC Press/Taylor & Francis (2017)
(84) J. Schoukens, G. Vandersteen, K. Barbé, and R. Pintelon: "Nonparametric preprocessing in system identification: A powerful tool", *Eur. J. Contr.*, 3-4:260–274 (2009)
(85) R. van der Maas, A. van der Maas, R. Voorhoeve, and T. Oomen: "Accurate FRF identification of LPV systems: nD-LPM with application to a medical X-ray system", *IEEE Trans. Contr. Syst. Techn.*, Vol.25, No.4, pp.1724–1735 (2017)
(86) R. Voorhoeve, A. van der Maas, and T. Oomen: "Non-parametric identification of multivariable systems: A local rational modeling approach with application to a vibration isolation benchmark", *Mech. Syst. Sign. Proc.*, To Appear.
(87) E. Rogers, K. Galkowski, and D.H. Owens: "Control Systems Theory and Applications for Linear Repetitive Processes", Number 349 in LNCIS. Springer, Berlin, Germany (2007)
(88) R.W. Longman: "Iterative learning control and repetitive control for engineering practice", *Int. J. Contr.*, Vol.73, No.10, pp.930–954 (2000)
(89) G. Pipeleers, B. Demeulenaere, and J. Swevers: "Optimal Linear Controller Design for Periodic Inputs", volume 394 of *LNCIS*, Springer, London, UK (2009)
(90) J. Bolder, T. Oomen, S. Koekebakker, and M. Steinbuch: "Using iterative learning control with basis functions to compensate medium deformation in a wide-format inkjet printer", *Mechatronics*, Vol.24, No.8, pp.944–953 (2014)
(91) J. Bolder and T. Oomen: "Inferential iterative learning control: A 2D-system approach", *Automatica*, Vol.71, pp.247–253 (2016)
(92) J. Wallén Axehill, I. Dressler, S. Gunnarsson, and A. Robertsson: "Estimation-based ILC applied to a parallel kinematic robot", *Contr. Eng. Prac.*, Vol.33, pp.1–9 (2014)
(93) L. Blanken, S. Koekebakker, and T. Oomen: "Design and modeling aspects in multivariable iterative learning control", In Proc. 55th Conf. Dec. Contr., pp.5502–5507, Las Vegas, NV, USA (2016)
(94) J. van Zundert and T. Oomen: "On inversion-based approaches for feedforward and ILC", *Mechatronics*, To appear.
(95) J. van Zundert, J. Bolder, S. Koekebakker, and T. Oomen: "Resource-efficient ILC for LTI/LTV systems through LQ tracking and stable inversion: Enabling large tasks on a position-dependent industrial printer", *Mechatronics*, Vol.38, pp.76–90 (2016)
(96) R. de Rozario, T. Oomen, and M. Steinbuch: "ILC and feedforward control for LPV systems: with application to a position-dependent motion system",

In Proc. 2017 Americ. Contr. Conf., pp.3518–3523, Seattle, WA, USA (2017)
(97) J. van Zundert and T. Oomen: "An approach to stable inversion of lptv systems with application to a position-dependent motion system", In Proc. 2017 Americ. Contr. Conf., pp.4890–4895, Seattle, WA, USA (2017)
(98) S. Mishra, W. Yeh, and M. Tomizuka: "Iterative learning control design for synchronization of wafer and reticle stages", In Proc. 2008 Americ. Contr. Conf., pp.3908–3913, Seattle, WA, USA (2008)
(99) J. van de Wijdeven and O. Bosgra: "Using basis functions in iterative learning control: Analysis and design theory", *Int. J. Contr.*, Vol.83, No.4, pp.661–675 (2010)
(100) M. Heertjes, D. Hennekens, and M. Steinbuch: "MIMO feed-forward design in wafer scanners using a gradient approximation-based algorithm", *Contr. Eng. Prac.*, Vol.18, No.5, pp.495–506 (2010)
(101) D.J. Hoelzle, A.G. Alleyne, and A.J. Wagoner Johnson: "Basis task approach to iterative learning control with applications to micro-robotic deposition", *IEEE Trans. Contr. Syst. Techn.*, Vol.19, No.5, pp.1138–1148 (2011)
(102) L. Blanken, F. Boeren, D. Bruijnen, and T. Oomen: "Batch-to-batch rational feedforward control: from iterative learning to identification approaches, with application to a wafer stage", *IEEE Trans. Mech.*, Vol.22, No.2, pp.826–837 (2017)
(103) F. Boeren, D. Bruijnen, N. van Dijk, and T. Oomen: "Joint input shaping and feedforward for point-to-point motion: Automated tuning for an industrial nanopositioning system", *Mechatronics*, Vol.24, No.6, pp.572–581 (2014)
(104) J. Bolder and T. Oomen: "Rational basis functions in iterative learning control - with experimental verification on a motion system", *IEEE Trans. Contr. Syst. Techn.*, Vol.23, No.2, pp.722–729 (2015)
(105) J. van Zundert, J. Bolder, and T. Oomen: "Optimality and flexibility in iterative learning control for varying tasks", *Automatica*, Vol.67, pp.295–302 (2016)
(106) L. Blanken, G. Isil, S. Koekebakker, and T. Oomen: "Flexible ILC: Towards a convex approach for non-causal rational basis functions", In IFAC 2017 Triennial World Congress, pp.12613–12618, Toulouse, France (2017)
(107) J. van Zundert and T. Oomen: "Inverting nonminimum-phase systems from the perspectives of feedforward and ILC", In IFAC 2017 Triennial World Congress, pp.12607–12612, Toulouse, France (2017)
(108) S. Devasia, D. Chen, and B. Paden: "Nonlinear inversion-based output tracking", *IEEE Trans. Automat. Contr.*, Vol.41, No.7, pp.930–942 (1996)
(109) W. Ohnishi and H. Fujimoto: "Tracking control method for plant with continuous time unstable zeros—stable inversion by time axis reversal and multirate feedforward—", In IEE of Japan Technical Meeting Record, pp.109–114 (2015) MEC-15-047.
(110) F. Boeren, D. Bruijnen, and T. Oomen: "Enhancing feedforward controller tuning via instrumental variables: With application to nanopositioning", *Int. J. Contr.*, Vol.90, No.4, pp.746–764 (2017)
(111) F. Boeren, L. Blanken, D. Bruijnen, and T. Oomen: "Optimal estimation of rational feedforward controllers: An instrumental variable approach and noncausal implementation on a wafer stage", *Asian J. Contr.*, Vol.20, No.1, pp.1–18 (2018)
(112) T. Söderström and P.G. Stoica: Instrumental Variable Methods for System Identification, volume 57 of LNCIS, Springer-Verlag, Berlin, Germany (1983)
(113) S. Devasia, E. Eleftheriou, and S. Moheimani: "A survey of control issues in nanopositioning", *IEEE Trans. Contr. Syst. Techn.*, Vol.15, No.5, pp.802–823 (2007)
(114) S. Moheimani and E. Eleftheriou: "Dynamics and control of micro- and nanoscale systems", *IEEE Contr. Syst. Mag.*, Vol.33, No.6, pp.42–45 (2013)
(115) G. Cherubini, C.C. Chung, W.C. Messner, and S. Moheimani: "Introduction to the special section on advanced servo control for emerging data storage systems", *IEEE Trans. Contr. Syst. Techn.*, Vol.20, No.2, pp.292–295 (2012)
(116) D.Y. Abramovitch: "Trying to keep it real: 25 years of trying to get the stuff I learned in grad school to work on mechatronic systems", In Proc. 2015 Multi-conf. Syst. Contr., pp.223–250, Syndey, Australia (2015)
(117) S. Van Huffel, V. Sima, A. Varga, S. Hammarling, and F. Delebecque: "High-performance numerical software for control", *IEEE Contr. Syst. Mag.*, Vol.24, No.1, pp.60–76 (2004)
(118) T. Oomen and C.R. Rojas: "Sparse iterative learning control with application to a wafer stage: Achieving performance, resource efficiency, and task flexibility", *Mechatronics*, Vol.47, pp.134–137 (2017)
(119) S. Galeani, S. Tarbouriech, M. Turner, and L. Zaccarian: "A tutorial on modern anti-windup design", *Eur. J. Contr.*, Vol.15, No.3-4, pp.418–440 (2009)
(120) M.F. Heertjes: "Variable gain motion control of wafer scanners", *IEEJ Journal of Industry Applications*, Vol.5, No.2, pp.90–100 (2016)
(121) M. Steinbuch, J. van Helvoort, W. Aangenent, B. de Jager, and R. van de Molengraft: "Data-based control of motion systems", In Proc. 2005 Americ. Contr. Conf., pp.529–534, Toronto, Canada (2005)
(122) J. van Zundert, T. Oomen, D. Goswami, and W. Heemels: "On the potential of lifted domain feedforward controllers with a periodic sampling sequence", In Proc. 2016 Americ. Contr. Conf., pp.4227–4232, Boston, MA, USA (2016)
(123) H. Fujimoto, Y. Hori, and A. Kawamura: Perfect tracking control based on multirate feedforward control with generalized sampling periods", *IEEE Trans. Ind. Electr.*, Vol.48, No.3, pp.636–644 (2001)
(124) S. Formentin, K. van Heusden, and A. Karimi: "A comparison of model-based and data-driven controller tuning", *Int. J. Adapt. Contr. Sign. Proc.*, Vol.28, No.10, pp.882–897 (2014)
(125) M. Heertjes, B. van der Velden, and T. Oomen: "Constrained iterative feedback tuning for robust control of a wafer stage system", *IEEE Trans. Contr. Syst. Techn.*, Vol.24, No.1, pp.56–66 (2016)
(126) P. Janssens, G. Pipeleers, and J. Swevers: "A data-driven constrained norm-optimal iterative learning control framework for LTI systems", *IEEE Trans. Contr. Syst. Techn.*, Vol.21, No.2, pp.546–551 (2013)
(127) J. Bolder, S. Kleinendorst, and T. Oomen: "Data-driven multivariable ILC: Enhanced performance by eliminating L and Q filters", *Int. J. Rob. Nonlin. Contr.*, To appear.

Tom Oomen (Non-member) received the M.Sc. degree (cum laude) and Ph.D. degree from the Eindhoven University of Technology, Eindhoven, The Netherlands. He held visiting positions at KTH, Stockholm, Sweden, and at The University of Newcastle, Australia. Presently, he is an assistant professor with the Department of Mechanical Engineering at the Eindhoven University of Technology. He is a recipient of the Corus Young Talent Graduation Award, the 2015 IEEE Transactions on Control Systems Technology Outstanding Paper Award, and the 2017 IFAC Mechatronics Best Paper Award. He is Associate Editor on the IEEE Conference Editorial Board, IFAC Mechatronics, and the IEEE Control Systems Letters (L-CSS). His research interests are in the field of system identification, robust control, and learning control, with applications in mechatronic systems.